RESEARCH ARTICLE

Interdependence between bacterial EPS and early grain coat development

Dimitrios Charlaftis[1] | Stuart J. Jones[1] | Lars Grimm[2] | Andreas Kappler[2]

[1]Department of Earth Sciences, Durham University, Durham, UK

[2]Geomicrobiology, Center for Applied Geosciences, University of Tuebingen, Tuebingen, Germany

Correspondence
Dimitrios Charlaftis, Department of Earth Sciences, Durham University, Durham DH1 3LE, UK.
Email: dimitrios.charlaftis@durham.ac.uk

Funding information
Durham University; Seedcorn

Abstract

Bacteria are the most abundant forms of life we know on our planet, able to survive in a variety of habitats, that play an important role in mineral formation and transformation processes. Here, we present laboratory experiments in which unconsolidated quartz grains were seeded with *Geobacter sulfurreducens* cells and exposed to a mineral medium solution for 96 hours at temperatures of between 60°C and 120°C. Experimental data show the interdependence between extracellular polymeric substances (EPS) and the early formation of grain-coating material. The occurrence of EPS promotes the development of web and bridging structures binding the quartz grains and creating EPS-coated surfaces. With increasing temperature, an amorphous mineral phase grows preferentially on these surfaces suggesting that EPS can act as a template for mineral nucleation. At temperatures >100°C, the order of crystallinity of the amorphous authigenic phase increases, transitioning to poorly-ordered rosette-like textures.

1 | INTRODUCTION

Grain-coating minerals in sandstones have been demonstrated as effective barriers preventing quartz cementation. Such minerals result from the transformation of precursor phases (Aagaard et al., 2000; Charlaftis et al., 2021) formed during deposition or soon afterward (Bloch et al., 2002). Detrital clay aggregates, potential sources for diagenetic coats, have been found on sand grains in modern estuarine environments (Dowey et al., 2017; Virolle et al., 2019) where bio-sediment interaction is prominent.

Microbial activity at the sediment–water interface promotes biofilm development. Biofilm is defined as an assemblage of microbial cells of various species, such as bacteria and microbial eukaryotes, attached to a surface in a matrix consisting of extracellular polymeric substances (EPS). EPS comprise organic molecules, mainly polysaccharides (Stoodley et al., 2002), are structurally and functionally essential for biofilm growth and involved in microbial adhesion to surfaces (Costa et al., 2018).

In estuarine and lagoonal settings, most sediment is composed of non-cohesive, unconsolidated sand grains. Biofilms provide important ecosystem functions, including sediment stabilization (Paterson et al., 2018; Vignaga et al., 2013), transportation, and bedform stabilization (Malarkey et al., 2015; Schindler et al., 2015). For example, diatom motility and adhesion in near-surface sediments are facilitated by sticky EPS strands bridging grain surfaces (Higgins et al., 2003). EPS contributes to sediment fabric by enhancing the cohesive forces between the sedimentary components (Van Colen et al., 2014).

Numerous studies document interactions between microbes and clay minerals and their importance in geological processes (Cuadros, 2017; Dong, 2012; Douglas & Beveridge, 1998; Folk & Lynch, 1997). A two-step process proposed for biogenic clay authigenesis includes the initial encrustation of iron that surrounds cells or filaments followed by Al-Si complexion (Konhauser et al., 1993). This initial cellularly-bound iron phase acts as a ligand that promotes the precipitation of an amorphous, poorly crystallized aluminosilicate phase engulfing the cell wall or EPS. Further mineralization results in more crystalline phases (Sánchez-Navas et al., 1998) tangentially oriented to the substratum (Konhauser & Urrutia, 1999). Ueshima and Tazaki (2001) showed that EPS of biofilms could serve

as a template for layer-silicate synthesis and catalyse the precipitation of iron-rich smectite.

Wooldridge et al. (2017) used chlorophyll-a as a proxy to show a positive correlation between sediment biofilm abundance and clay-coat coverage in intertidal estuarine sediments. Duteil et al. (2020) performed laboratory experiments producing clay-coated quartz sands by mixing EPS derived from intertidal diatom biofilms with clay minerals and quartz. These experiments are associated with microorganisms living in aquatic environments. However, close occurrence of biofilms and minerals can also be found in the soil microbiome.

In this study, we mixed single-species bacterial biofilms with high purity quartz sand samples, which were subsequently used in temperature-controlled laboratory experiments to address the following questions: (1) how do EPS of biofilms coat the sand grains, (2) do biofilms act as a growth surface, (3) is the stickiness of the biofilms the main reason for clays to coat the surface of quartz grains, and (4) does mineral authigenesis continue on biofilm surfaces only or expand on clean grain surfaces with increasing temperature. An artificial solution was used to grow and preserve the bacterial population and promoted mineral precipitation during each experiment.

Decoding the interdependence between bacterial EPS and early formation of grain-coating material has identified their importance for acting as a template for authigenic mineral growth.

2 | MATERIALS AND METHODS

The experimental process followed here is based on the following requirements: (1) to ensure the production of EPS that bridge and coat the quartz grains, (2) the artificial solution is enriched with the correct geochemical components to sustain biofilm growth and, with progressive temperature increase, allow mineral nucleation, and (3) besides their use as substrate material, quartz grains act as a silica source for authigenesis.

2.1 | Sand grains and microorganism cultivation

Unconsolidated high-purity quartz sand grains were used as a template for biofilm development. Biofilm growth was achieved using
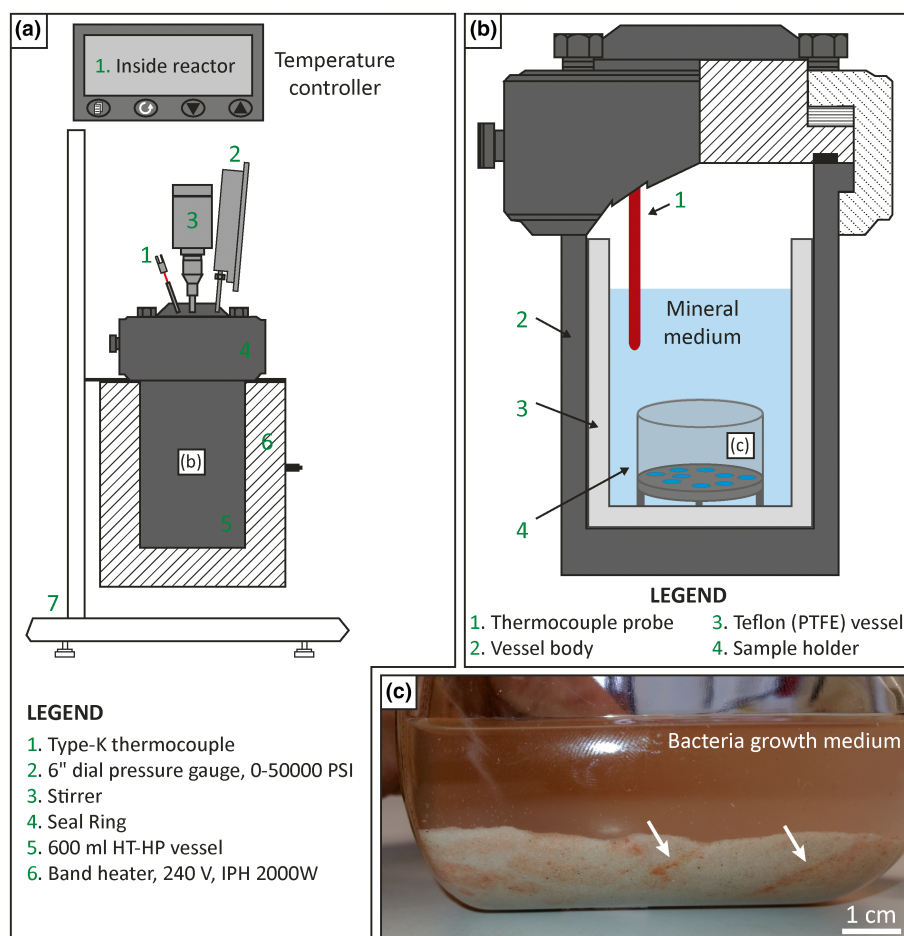

FIGURE 1 Illustration of the experimental setup. (a) Schematic representation of the hydrothermal vessel and its main parts utilized for the biofilm experiments. The system comprises solely stainless-steel components and a Eurotherm temperature control. (b) The interior of the hydrothermal vessel. (c) Pure sand grains seeded with *Geobacter sulfurreducens* cells. Note the biofilm (white arrows) development in between the sand particles.

Geobacter sulfurreducens, selected for their wide distribution in soils, freshwater and marine environments (Coates et al., 1996; Lonergan et al., 1996; Lovley et al., 2004). *Geobacter sulfurreducens* is an anaerobic microorganism capable of reducing e.g. Fe(III) minerals, elemental sulphur or fumarate with acetate as electron donor (Lovley et al., 2004). The bacterial strains were obtained from the laboratory culture collection of the Tuebingen Geomicrobiology Group.

The strains were cultivated in the dark under anoxic conditions (N_2:CO_2; 90:10 headspace) at 35°C in a modified mineral medium (Tables S1 and S2). Growth and cell concentration were monitored by optical density measurements at 600nm (OD600). Stationary phase cultures were harvested by centrifugation at 2800g at 10°C three times for 20min and washed with bicarbonate buffer (30mM, pH 6.8) to prepare a cell suspension with a final cell density of 10^9 cells/mL.

Subsequently, 10 mL of the cell suspension was dispensed in a newly prepared mineral medium (pH 6.8). 50g of pure quartz grains and 50mL of the new medium containing the strains were placed in 250mL serum bottles and left in the dark at 35°C for incubation. The bottles were manually rotated daily, keeping the quartz sand below the media surface to ensure biofilm development between sand grains (Figure 1c).

2.2 | Experimental setup

Hydrothermal reactor experiments were carried out in a Parr© Series 4560 Mini Reactor comprised of a cylindrical 316 stainless steel pressure vessel (600mL) under strictly closed conditions (Figure 1). Four experiments were performed at temperatures between 60°C and 120°C using 5 g of the pure sand grains seeded with *Geobacter* cells and 100mL of the mineral medium as pore fluid (see supplementary material). Although most bacteria thrive at lower temperatures in natural environments, the experimental temperature range was selected to include shallow burial (30–70°C) and mesodiagenetic (>70°C) temperature conditions (Morad et al., 2000), ensuring mineral growth within the experimental timeframe. Based on a geothermal gradient of 30°C km^{-1}, the experimental temperature range equates to a burial depth of between 2–4 km. All samples were held at the desired
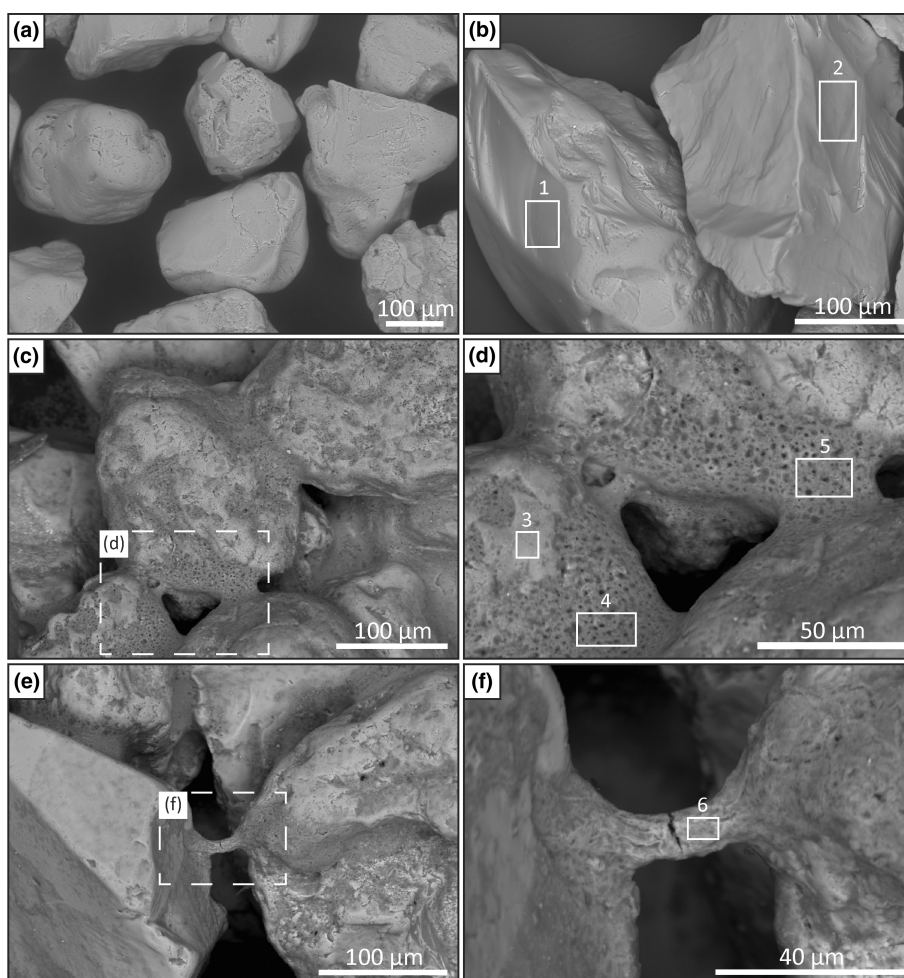

FIGURE 2 Pure sand (quartz) sample (starting material) before and after being seeded with *Geobacter sulfurreducens* cells forming biofilm structures. Diverse types of quartz grains were present. For the associated EDS analysis (e.g., spectrum 1–6) refer to Table 1. (a, b) SE image of the unconsolidated quartz grains (c) Binding of quartz grains by the extracellular polymeric substances (EPS) matrix of the biofilm structures. d) EPS web linking quartz grains. (e, f) Bridging structure between two quartz grains due to EPS strands.

TABLE 1 Quantification results of the SEM-EDS elemental analysis of spectrum 1–16 as shown in Figure 2–5.

Spectrum	Elements									
	O (%)	Si (%)	Na (%)	Mg (%)	Fe (%)	K (%)	Ca (%)	S (%)	Cl (%)	P (%)
1, 2	67.7 ±0	33.3 ±0	–	–	–	–	–	–	–	–
3	64.9 ±1.2	31.6 ±0.82	3.1 ±2.4	–	–	0.1 ±0.06	0.1 ±0.07	–	0.2 ±0.1	–
4	43.5 ±1.9	3.9 ±2.6	42.2 ±2.51	1.5 ±0.2	–	1.1 ±0.3	0.2 ±0.07	2.5 ±0.3	3.1 ±1	2 ±0.2
5	40.6 ±2.11	0.4 ±2.4	45.6 ±2.42	1.1 ±0.27	–	1.7 ±0.43	0.3 ±0.03	3 ±0.38	5.1 ±1.36	-
6	47.5 ±1.33	1.6 ±0.36	31.3 ±3.23	3.4 ±0.07	0.4 ±0.2	1.6 ±0.64	1.6 ±0.6	2.5 ±1.02	4.1 ±0.41	6 ±0.66
7	43.7 ±5.22	0.9 ±5.5	36.7 ±8.34	3.5 ±0.49	–	1.2 ±0.24	3.1 ±0.5	1.4 ±0.19	4.7 ±1.39	4.9 ±0.58
8	53 ±3.08	10.5 ±5.94	27.2 ±10.05	1.9 ±0.05	–	0.4 ±0.08	1.2 ±0.33	3.1 ±1.74	0.4 ±1.95	2.3 ±0.44
9	61.1 ±0.91	26 ±0.85	10.5 ±4.5	2.5 ±0.28	–	–	–	–	–	–
10	63.2 ±0.64	24 ±1.32	4 ±3.19	1.9 ±0.6	–	–	5.2 ±1.89	–	–	1.7 ±0.66
11	43.7 ±7.07	4.9 ±1.97	39.7 ±15.14	3.4 ±1.73	–	1 ±0.31	0.6 ±3.29	1.9 ±0.9	3.3 ±1.68	1.5 ±3.04
12	61.1 ±2.49	22.2 ±3.51	11.1 ±2.94	1.9 ±1.44	–	–	1.4 ±0.18	–	–	2.3 ±0.11
13	52.4 ±0.18	12.5 ±0.71	21.9 ±1.36	9 ±1.58	0.2 ±0.05	0.4 ±0.14	0.4 ±0.02	0.7 ±0.08	1.3 ±0.03	1.2 ±0.18
14	66.4 ±1.81	33.1 ±2.02	0.5 ±3.08	–	–	–	–	–	–	–
15	56.9 ±6.9	22.9 ±8.51	15.5 ±11.26	0.7 ±0.24	–	1.7 ±0.74	–	–	1.6 ±1.58	0.7 ±0.55
16	40.4 ±0.44	2.8 ±0.11	44.9 ±0.83	0.4 ±0.14	–	2.7 ±0.18	–	1.8 ±0.1	4.8 ±1.58	2.1 ±0

Note: All data are reported in atomic percent normalized to oxygen by stoichiometry. All errors are standard deviations.

experimental temperature for 96h. At the end of each experiment, the samples were removed from the vessel and air-dried.

2.3 | Analytical techniques

A Hitachi SU-70 field emission gun scanning electron microscope (SEM) equipped with an energy-dispersive detector (EDS) was used for rapid elemental identification of the new, due to the experimental treatment, mineral precipitates. The mineralogy of the samples was also evaluated by bulk and clay fraction (<2 μm fraction) X-ray powder diffraction (XRD) analysis.

Aqueous bulk solutions were analysed, using triple quadrupole inductively coupled plasma mass spectrometry (TQ ICP-MS), to establish the elemental composition before and after the experiments at 60°C, 80°C, and 100°C. Liquid fraction could not be obtained from the hydrothermal vessel after the experiment at 120°C as the solution was consumed by the reaction. For more information regarding each technique, see supplementary material.

3 | RESULTS

3.1 | Sand grains pre- and post-biofilm growth

The initial unconsolidated pure sand was composed of quartz grains (Figure 2) of subangular to subrounded shape and size ranging between 150 and 400μm. SEM imaging indicated that some grains showed smooth surfaces while others were etched and displayed conchoidal fractures.

Detailed EDS analysis (e.g., spectrum 1–6, Table 1) confirmed that the starting material is quartz (i.e., the elemental composition consists solely of Si and O) and shows the low Si content in regions of quartz surfaces covered by biological material. EPS connected to quartz grain surfaces developing webs (Figure 2c,d) and strands (Figure 2e,f) that link individual sand grains and bridge void space.

3.2 | Hydrothermally treated biofilm-rich sand samples

At 60°C, the EPS strands were preserved (Figure 3a,b), and spheroidal aggregates developed on the surface of host grains (Figure 3c). The SEM-EDS analysis indicated the presence of Mg in regions of quartz surfaces covered by the neoformed mineral precipitates. At 80°C, the formation of a phase that is morphologically similar to clay material was linked to EPS strands and webs (Figure 3d–f). Mineral growth was favoured at cavities and edged surfaces of the biocoated grains (Figure 3d,e). The crystals were strongly curled, and individual crystals could not be resolved. Rhombic-shaped dolomite crystals appeared mixed with the amorphous material as well as on EPS-free quartz grain surfaces (Figure 3d,f).

After the hydrothermal experiment at 100°C, the loose quartz grains transformed into a more rigid framework due to a change in the EPS texture associated with mineral growth (Figure 4a). The EPS strands were still preserved, and a thin layer of EPS coating several grains was observed (Figure 4b). Mineral precipitation occurred mainly in regions surrounding grains bounded by EPS (Figure 4c). The new precipitates were low-ordered structures with chemical compositions differing from the detrital material (Figure 4d).

At 120°C, quartz grains were partially coated by the neoformed mineral phase with strands and web structures, similar to those developed by the biofilm growth, being the primary targets
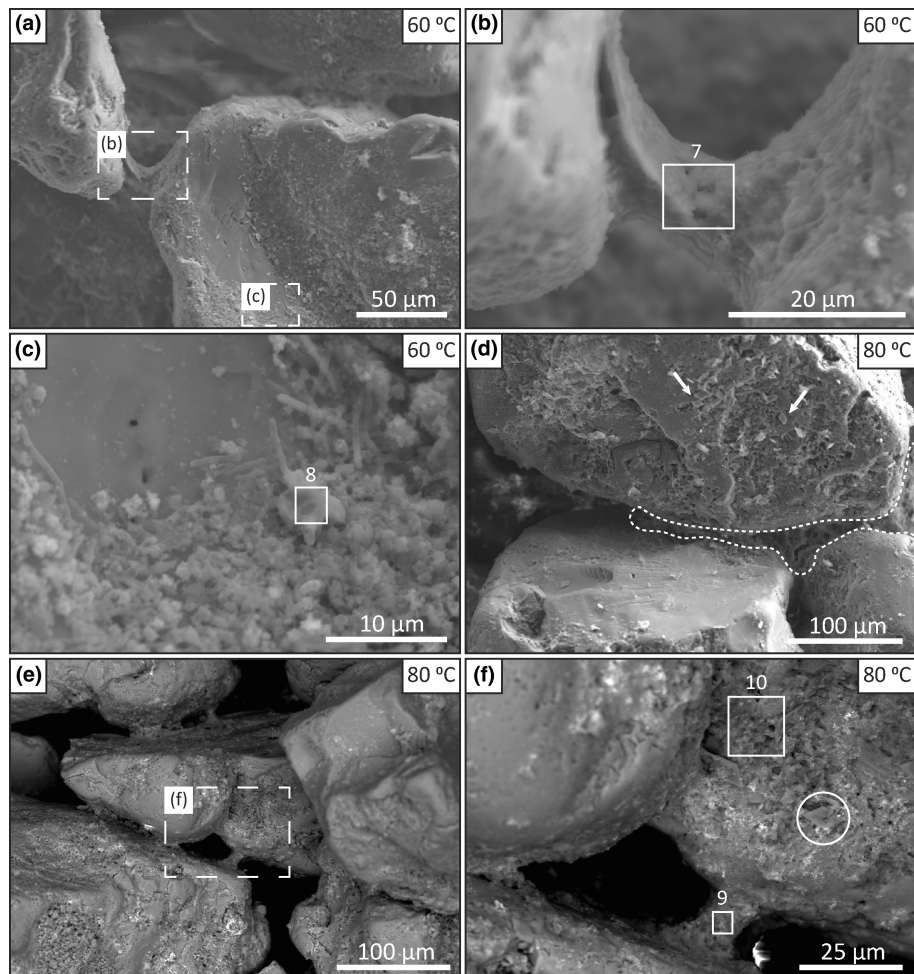
FIGURE 3 SEM photomicrographs of quartz grain samples with developed biofilm structures and neoformed mineral phases after hydrothermal treatment at 60°C (a–c) and 80°C (d–f). For the associated EDS analysis (e.g., spectrum 7–10) refer to Table 1. (a, b) Preserved EPS strands. c) Zoomed in area of (a) showing the spherical humps on the surface of the host grain. (d) SE image showing the contact between two quartz grains. Note the change in the texture of the binding material. Rhombic-shaped crystals developed on EPS-free quartz grain surfaces (arrows). (e) BSE image showing new mineral precipitates partially covering quartz grain surfaces. (f) BSE image showing the preservation of an EPS strand. Note the amorphous material adjacent to the contact between the quartz grains and the rhombic-shaped crystals (circle) blended in the amorphous phase after the hydrothermal treatment.

(Figure 5a,f). Sharp contacts between clean quartz surfaces and the regions covered by the grain-coating material were prominent. Rosette-like textures, indicative of an increase of the order of crystallinity, were observed (Figure 5c).

3.3 | Sample mineralogy and aqueous solution

Whole-rock XRD and <2 μm fraction analysis of the pre-experiment samples validated that the starting material was composed solely of quartz. Clay-separate analysis could not identify the morphologically clay-like material observed under the SEM. This is likely due to the lack of abundance of the newly precipitated phase either because the amount precipitated was insufficient to be captured by this technique or due to the nature of the phase (e.g., grain-coating) that, even after the ultrasound and centrifugation separation treatment, remained attached to the grains and did not make it into the analysis. However,

traces of dolomite were identified at temperatures >60°C, occurring as rhombic-shaped crystals observed under the SEM (Figure S1).

The greatest elemental concentration change of the analysed fluid samples was observed in the concentration of Mg and Ca, with values decreasing from 48,493.2 μg/L to 995.9 μg/L and 2587.9 μg/L to 9.2 μg/L, respectively (Table 2). A similar decreasing trend is followed by Fe, whereas Na and K remained relatively constant throughout the experiments.

4 | DISCUSSION

4.1 | EPS and grain stabilization

Biological cohesion occurs where EPS are secreted by microorganisms that inhabit natural sediments forming biofilms at the sediment surface. The EPS matrix prevents sand grains from moving independently

TABLE 2 Elemental analysis of the mineral medium at each experimental stage between 0 (e.g., pre-exp) and 100°C.

Element	Experimental temperature (°C)			
	0	60	80	100
B	105.8	136.4	139.9	137.9
Na	3,015,082.3	3,744,446.8	3,564,936.0	4,221,123.9
Mg	48,493.2	51,359.1	25,017.3	995.9
K	174,499.6	226,379.6	209,346.6	248,416.7
Ca	2587.9	1621.1	887.1	9.2
Mn	11.0	59.2	14.9	0.6
Fe	31.3	12.4	4.3	0.2
Co	38.7	30.6	20.7	8.8
Ni	7.7	132.2	1089.3	244.8
Cu	0.8	7.6	39.8	11.3
Zn	29.6	42.7	18.2	9.3
Se	0.6	0.6	0.8	1.1
Mo	14.0	62.8	1292.4	770.2
W	0.1	1.1	18.6	16.0

Note: Highlighted in green are the elements showing the biggest change that are also commonly associated with clay mineral and carbonate cements. Elemental concentrations are reported in µg/L.
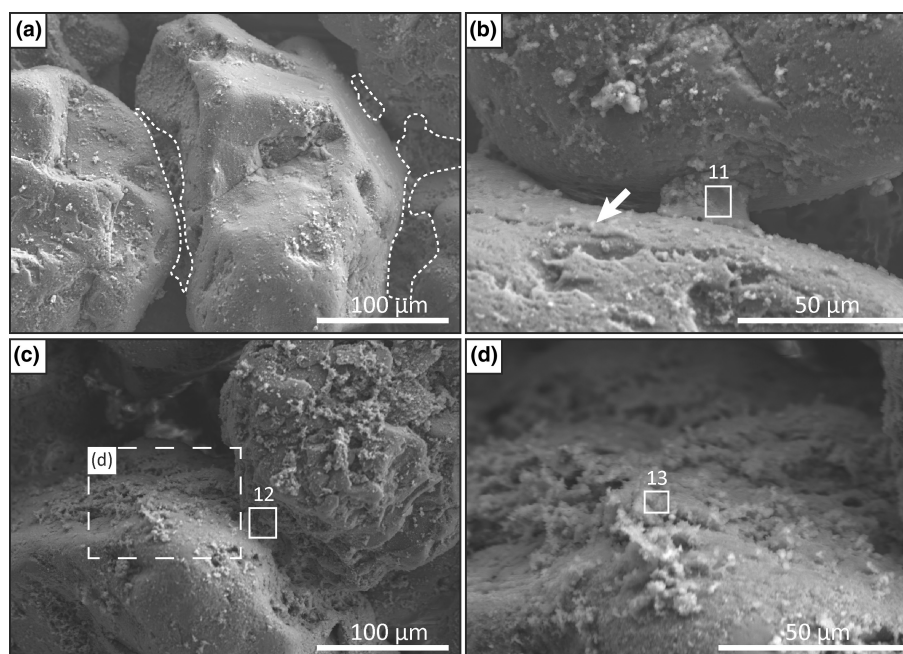

FIGURE 4 SEM photomicrographs after hydrothermal treatment at 100 °C. For the associated EDS analysis (e.g., spectrum 11–13) refer to Table 1. (a) The binding of quartz grains (outlined) remains unaltered. (b) Only small strands are preserved. Note the presence of a thin EPS layer covering the surface of a grain (arrow). (c, d) Microcrystalline material in close proximity to EPS binding two quartz grains.

by creating bonds between them (Decho, 2000). Our initial experiment of seeding pure sand grains with *Geobacter* cells demonstrates that biofilm colonization preferentially happens on quartz substratum with abraded surfaces and points of contact between grains. After the successful adhesion and attachment, further biofilm growth is controlled by the adsorption of dissolved constituents and sufficient nutrient provision from the artificial aqueous environment.

At near-neutral pH, EPS have a net negative charge on their surface produced by carboxylic, hydroxyl and phosphoryl groups so that they can attract and retain cation species (Cuadros, 2017). The presence of monovalent (Na^+) and divalent (Ca^{2+}, Mg^{2+}) cations in the mineral medium (pH = 6.8) used potentially helped in bridging negatively charged groups within polymers and between the different surfaces of bacteria and sand particles, leading to biostabilization (de Brouwer et al., 2002; Flemming & Wingender, 2010). Interactions between EPS and the surface of quartz grains could result from electrostatic bonds formed between charged groups of EPS and silanol groups (Tang et al., 2015). Additionally, the biocolonization of the
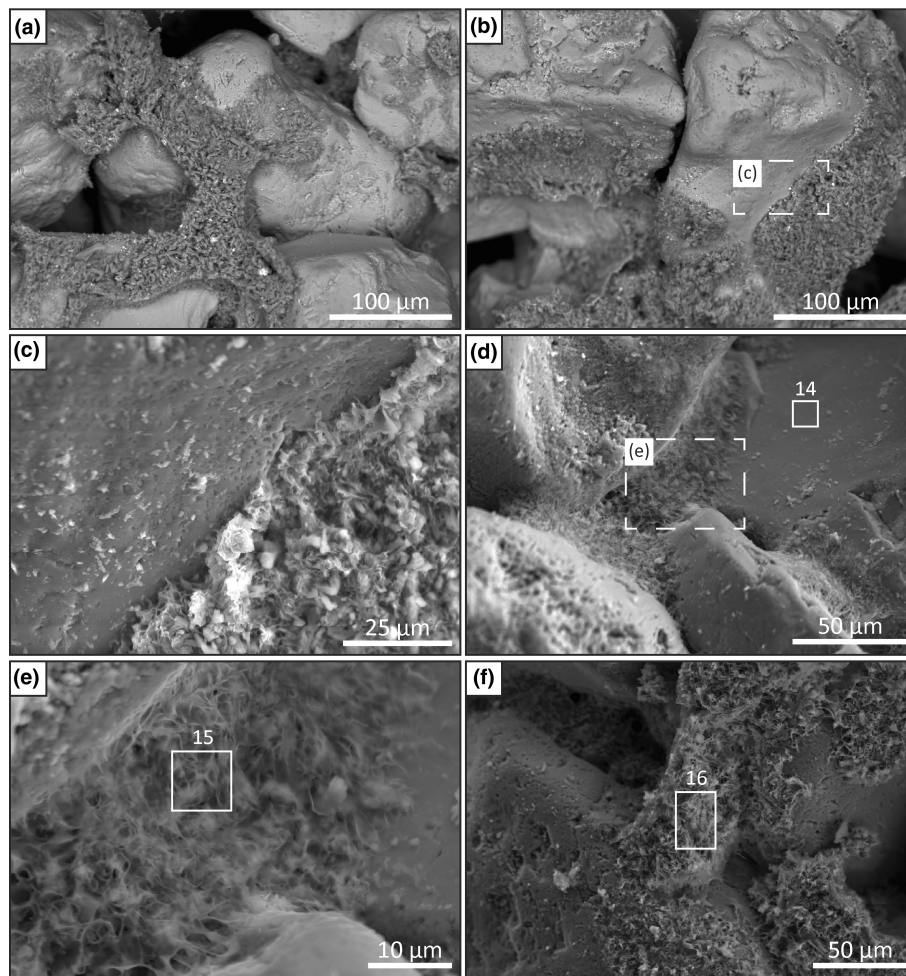
FIGURE 5 SEM photomicrographs showing the interrelation of biofilm structures and neoformed mineral phases after hydrothermal treatment at 120°C. For the associated EDS analysis (e.g., spectrum 14–16) refer to Table 1. (a) BSE image showing the precipitated mineral that forms a web linking quartz grains. The EPS web developed before the experiment possibly acted as a nucleation substrate for the precipitation of the new mineral. (b, c) The mineral selectively coats specific regions of the grain, further promoting the hypothesis that mineral authigenesis begins from regions previously coated by EPS. Note the presence of rosette-like clusters. (d, e) Mineral authigenesis occurred between quartz grains bounded by EPS before the experiment. (f) Strand with extensive mineral growth bridging two quartz grains.

unconsolidated sand grains occurred in conditions with low energy impact (i.e., low hydraulic conditions and low mobility of sand grains). This allowed the bacteria to produce and sustain the observed cohesive bio-coating and bridging structures.

4.2 | Association of EPS with mineral formation

Bacteria biomineralization is dependent upon the chemical composition of the waters in which the microorganisms are growing (Konhauser et al., 1998). Biofilms, owing to their chemical reactivity and large surface area, are considered ideal scavengers of metal cations (Geesey et al., 1988). In our experiments, Mg and Ca cations were bound by the surface of the polymers. The continued adsorption results in surface site saturation, and once critical supersaturation has been reached, critical nuclei become established. With increasing temperature and appropriate geochemical components provided by the mineral medium, mineral growth continues

abiogenically transitioning from an initial amorphous phase to a low order crystalline material with rosette-like textures (Figure 5c).

Except for the morphologically clay-like phase, rhombic-shaped dolomite crystals were also observed; however, their abundance was volumetrically less significant. The limited abundance of the dolomite crystals can be attributed to the fact that amorphous phases have lower interfacial free energies, with a faster nucleation rate than those of more stable, crystalline phases. As a result, Mg is primarily used by the clay-like phase, thus preventing extensive calcium carbonate precipitation on the EPS-coated surfaces. This could also explain why dolomite is sporadically found on EPS-free quartz grain surfaces (Figure 3d).

4.3 | Limitations of the present study and future work

Natural early diagenetic conditions cannot be fully reproduced in the laboratory due to the short experimental time compared to a

geological timeframe and uncertainties associated with the chosen aqueous chemistry. Further experiments remain to be performed to improve the applied experimental procedure and develop a more comprehensive understanding of these initial findings. Prolonged experimental times will help to better constrain the mineralogy of the newly formed grain-coating mineral. The introduction of pressure dependency in such experiments is also important as elevated pressures have a marked effect on the stability of authigenic minerals during burial diagenesis. Additionally, since the identity of the organic compounds in the biofilm plays a key role for the interaction of the cells with the mineral particles, determining the composition and spatial distribution of the molecules in the organic biofilm matrix could be an additional future target.

The procedure can be repeated using a mixture of reference clay minerals with high-purity quartz grains as a starting substrate for bacteria cultivation and further hydrothermal treatment. From the technical perspective, advanced imaging techniques such as X-ray computed tomography, cryogenic focused ion beam scanning electron microscopy and cryo-transmission electron microscopy can be used to maintain samples in as near-to-native as state as possible, hence deciphering the structure of potential mineralized bacteria and stages of biomineralization.

5 | CONCLUSIONS

1. Unconsolidated high-purity sand grains were used as a template for the development of bacterial biofilm. Biofilm growth was laboratory synthesized using *Geobacter sulfurreducens* cells and a modified mineral medium. Subsequently, the biofilm-rich sands were hydrothermally treated at temperatures between 60°C and 120°C simulating diagenetic conditions. This research has experimentally demonstrated the interaction between bacterial EPS and grain-coating authigenesis.

2. The experimental results provide evidence of the ability of synthesized bacterial EPS surfaces to serve as templates for mineral synthesis. Formation of an amorphous mineral phase, that is morphologically similar to a poorly developed clay mineral phase, and dolomite crystals was induced by the adsorption of Mg and Ca cations from the EPS surface and further interaction with silicate anions.

3. With increasing temperature, the crystallinity of the amorphous phase increased. Rosette textures were observed at temperatures >100°C. Dolomite crystals precipitated on EPS-free surfaces.

4. These initial findings enhance our understanding on the formation of thinly layered grain-coating material resembling precursor phases that can potentially govern later diagenetic processes.

REFERENCES

Aagaard, P., Jahren, J. S., Harstad, A. O., Nilsen, O., & Ramm, M. (2000). Formation of grain-coating chlorite in sandstones. Laboratory synthesized vs. natural occurrences. *Clay Minerals*, *35*(1), 261–269. https://doi.org/10.1180/000985500546639

Bloch, S., Lander, R. H., & Bonnell, L. (2002). Anomalously high porosity and permeability in deeply buried sandstone reservoirs: Origin and predictability. *AAPG Bulletin*, *86*(2), 301–328. https://doi.org/10.1306/61EEDABC-173E-11D7-8645000102C1865D

Charlaftis, D., Jones, S. J., Dobson, K. J., Crouch, J., & Acikalin, S. (2021). Experimental study of chlorite authigenesis and influence on porosity maintenance in sandstones. *Journal of Sedimentary Research*, *91*(2), 197–212. https://doi.org/10.2110/jsr.2020.122

Coates, J. D., Phillips, E. J., Lonergan, D. J., Jenter, H., & Lovley, D. R. (1996). Isolation of Geobacter species from diverse sedimentary environments. *Applied and Environmental Microbiology*, *62*(5), 1531–1536.

Costa, O. Y. A., Raaijmakers, J. M., & Kuramae, E. E. (2018). Microbial extracellular polymeric substances: Ecological function and impact on soil aggregation. *Frontiers in Microbiology*, *9*, 1636. https://doi.org/10.3389/fmicb.2018.01636

Cuadros, J. (2017). Clay mineral interaction with microorganisms: A review. *Clay Minerals*, *52*, 235–261.

de Brouwer, J. F. C., Ruddy, G. K., Jones, T. E. R., & Stal, L. J. (2002). Sorption of EPS to sediment particles and the effect on the rheology of sediment slurries. *Biogeochemistry*, *61*(1), 57–71. https://doi.org/10.1023/A:1020291728513

Decho, A. W. (2000). Microbial biofilms in intertidal systems: An overview. *Continental Shelf Research*, *20*(10), 1257–1273. https://doi.org/10.1016/S0278-4343(00)00022-4

Dong, H. (2012). Clay–microbe interactions and implications for environmental mitigation. *Elements*, *8*(2), 113–118. https://doi.org/10.2113/gselements.8.2.113

Douglas, S., & Beveridge, T. J. (1998). Mineral formation by bacteria in natural microbial communities. *FEMS Microbiology Ecology*, *26*(2), 79–88. https://doi.org/10.1111/j.1574-6941.1998.tb00494.x

Dowey, P. J., Worden, R. H., Utley, J., & Hodgson, D. M. (2017). Sedimentary controls on modern sand grain coat formation. *Sedimentary Geology*, *353*, 46–63. https://doi.org/10.1016/j.sedgeo.2017.03.001

Duteil, T., Bourillot, R., Grégoire, B., Virolle, M., Brigaud, B., Nouet, J., Braissant, O., Portier, E., Féniès, H., Patrier, P., Gontier, E., Svahn, I., & Visscher, P. T. (2020). Experimental formation of clay-coated sand grains using diatom biofilm exopolymers. *Geology*, *48*(10), 1012–1017. https://doi.org/10.1130/G47418.1

Flemming, H.-C., & Wingender, J. (2010). The biofilm matrix. *Nature Reviews Microbiology*, *8*(9), 623–633. https://doi.org/10.1038/nrmicro2415

Folk, R. L., & Lynch, F. L. (1997). The possible role of nannobacteria (dwarf bacteria) in clay-mineral diagenesis and the importance of careful sample preparation in high-magnification SEM study. *Journal of Sedimentary Research*, *67*(3), 583–589. https://doi.org/10.1306/d42685db-2b26-11d7-8648000102c1865d

Geesey, G. G., Jang, L., Jolley, J. G., Hankins, M. R., Iwaoka, T., & Griffiths, P. R. (1988). Binding of metal ions by extracellular polymers of biofilm bacteria. *Water Science and Technology*, *20*(11–12), 161–165. https://doi.org/10.2166/wst.1988.0279

Higgins, M. J., Molino, P., Mulvaney, P., & Wetherbee, R. (2003). The structure and nanomechanical properties of the adhesive mucilage that mediates diatom-substratum adhesion and motility1. *Journal of Phycology*, *39*(6), 1181–1193. https://doi.org/10.1111/j.0022-3646.2003.03-027.x

Konhauser, K. O., Fisher, Q. J., Fyfe, W. S., Longstaffe, F. J., & Powell, M. A. (1998). Authigenic mineralization and detrital clay binding by freshwater biofilms: The Brahmani river, India. *Geomicrobiology Journal*, *15*(3), 209–222. https://doi.org/10.1080/01490459809378077

Konhauser, K. O., Fyfe, W. S., Ferris, F. G., & Beveridge, T. J. (1993). Metal sorption and mineral precipitation by bacteria in two Amazonian river systems: Rio Solimões and Rio Negro, Brazil. *Geology*, *21*(12), 1103–1106. https://doi.org/10.1130/0091-7613(1993)021<1103:msampb>2.3.co;2

Konhauser, K. O., & Urrutia, M. (1999). Bacterial clay authigenesis: A common biogeochemical process. *Chemical Geology*, *161*(4), 399–413. https://doi.org/10.1016/S0009-2541(99)00118-7

Lonergan, D. J., Jenter, H. L., Coates, J. D., Phillips, E. J., Schmidt, T. M., & Lovley, D. R. (1996). Phylogenetic analysis of dissimilatory Fe(III)-reducing bacteria. *Journal of Bacteriology*, *178*(8), 2402–2408. https://doi.org/10.1128/jb.178.8.2402-2408.1996

Lovley, D. R., Holmes, D. E., & Nevin, K. P. (2004). Dissimilatory Fe(III) and Mn(IV) reduction. *Advances in Microbial Physiology*, *49*, 219–286. Academic Press.

Malarkey, J., Baas, J. H., Hope, J. A., Aspden, R. J., Parsons, D. R., Peakall, J., Paterson, D. M., Schindler, R. J., Ye, L., Lichtman, I. D., Bass, S. J., Davies, A. G., Manning, A. J., & Thorne, P. D. (2015). The pervasive role of biological cohesion in bedform development. *Nature Communications*, *6*(1), 6257. https://doi.org/10.1038/ncomms7257

Morad, S., Ketzer, J. M., & De Ros, L. F. (2000). Spatial and temporal distribution of diagenetic alterations in siliciclastic rocks: Implications for mass transfer in sedimentary basins. *Sedimentology*, *47*(s1), 95–120. https://doi.org/10.1046/j.1365-3091.2000.00007.x

Paterson, D. M., Hope, J. A., Kenworthy, J., Biles, C. L., & Gerbersdorf, S. U. (2018). Form, function and physics: The ecology of biogenic stabilisation. *Journal of Soils and Sediments*, *18*(10), 3044–3054. https://doi.org/10.1007/s11368-018-2005-4

Sánchez-Navas, A., Martín Algarra, A., & Nieto, F. (1998). Bacterially-mediated authigenesis of clays in phosphate stromatolites. *Sedimentology*, *45*(3), 519–533.

Schindler, R. J., Parsons, D. R., Ye, L. P., Hope, J. A., Baas, J. H., Peakall, J., Manning, A. J., Aspden, R. J., Malarkey, J., Simmons, S., Paterson, D. M., Lichtman, I. D., Davies, A. G., Thorne, P. D., & Bass, S. J. (2015). Sticky stuff: Redefining bedform prediction in modern and ancient environments. *Geology*, *43*(5), 399–402. https://doi.org/10.1130/g36262.1

Stoodley, P., Sauer, K., Davies, D. G., & Costerton, J. W. (2002). Biofilms as complex differentiated communities. *Annual Review of Microbiology*, *56*(1), 187–209. https://doi.org/10.1146/annurev.micro.56.012302.160705

Tang, C., Zhu, J., Li, Z., Zhu, R., Zhou, Q., Wei, J., He, H., & Tao, Q. (2015). Surface chemistry and reactivity of SiO2 polymorphs: A comparative study on α-quartz and α-cristobalite. *Applied Surface Science*, *355*, 1161–1167. https://doi.org/10.1016/j.apsusc.2015.07.214

Ueshima, M., & Tazaki, K. (2001). Possible role of microbial polysaccharides in nontronite formation. *Clays and Clay Minerals*, *49*(4), 292–299. https://doi.org/10.1346/ccmn.2001.0490403

Van Colen, C., Underwood, G. J. C., Serôdio, J., & Paterson, D. M. (2014). Ecology of intertidal microbial biofilms: Mechanisms, patterns and future research needs. *Journal of Sea Research*, *92*, 2–5. https://doi.org/10.1016/j.seares.2014.07.003

Vignaga, E., Sloan, D. M., Luo, X., Haynes, H., Phoenix, V. R., & Sloan, W. T. (2013). Erosion of biofilm-bound fluvial sediments. *Nature Geoscience*, *6*(9), 770–774. https://doi.org/10.1038/ngeo1891

Virolle, M., Brigaud, B., Bourillot, R., Féniès, H., Portier, E., Duteil, T., Nouet, J., Patrier, P., & Beaufort, D. (2019). Detrital clay grain coats in estuarine clastic deposits: Origin and spatial distribution within a modern sedimentary system, the Gironde estuary (south-West France). *Sedimentology*, *66*(3), 859–894. https://doi.org/10.1111/sed.12520

Wooldridge, L. J., Worden, R. H., Griffiths, J., Thompson, A., & Chung, P. (2017). Biofilm origin of clay-coated sand grains. *Geology*, *45*(10), 875–878. https://doi.org/10.1130/G39161.1

SUPPORTING INFORMATION

Additional supporting information can be found online in the Supporting Information section at the end of this article.
Appendix S1.